

SEARCHES FOR STRONG PRODUCTION OF SUPERSYMMETRIC PARTICLES

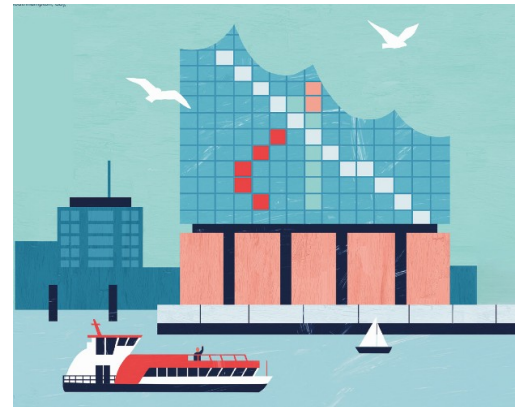


Stockholm
University



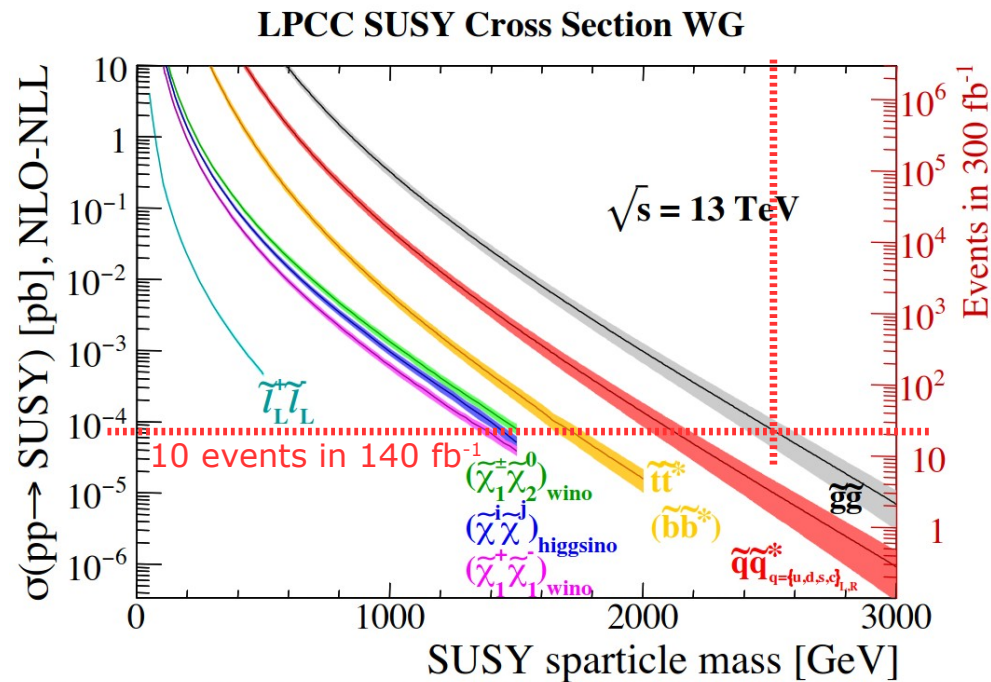
Sara Strandberg
on behalf of the ATLAS Collaboration

EPS-HEP, Hamburg, 24 August 2023



SUSY search program at the LHC

- SUSY has the potential to
 - provide a dark matter candidate;
 - unify the forces at high energy;
 - solve the fine-tuning problem of the Higgs mass.
- Broad search program to ensure that we get the most out of the LHC data.
 - Strong and electroweak production.
 - R-parity conserved and violated.
- Simplified models used for optimization and model-dependent exclusion limits.
 - Masses of non-relevant SUSY particles put very high.
 - 100% BR to specific final state.
- Check coverage in large pMSSM scans.
- Model-independent upper limits, HEP data, ...



<https://twiki.cern.ch/twiki/bin/view/LHCPhysics/SUSYCrossSections>

arXiv:1407.5066

- All results presented today with the 139-140 fb^{-1} of LHC Run-2 data.
- Limits on strongly produced SUSY particles can reach up to about 2.5 TeV.

Latest results from ATLAS in strong SUSY production

- Gluino production in multi-b final states **SUSY-2018-30**
- Gluino and squark production in multi-lepton final states **SUSY-2020-27**
- Stop production in $tt+E_T^{\text{miss}}$ final states **ATLAS-CONF-2023-043** **NEW**
- Stop production in $tc+E_T^{\text{miss}}$ final states **ATLAS-CONF-2023-058** (see J. Montejo Berlingen's talk) **NEW**

ATLAS SUSY Searches* - 95% CL Lower Limits

March 2023

ATLAS Preliminary

$\sqrt{s} = 13 \text{ TeV}$

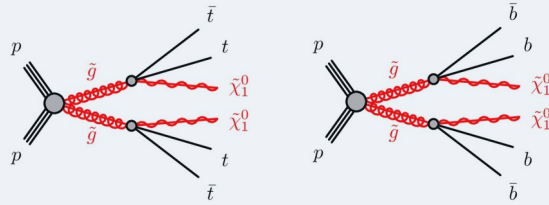
Model	Signature	$\int \mathcal{L} dt [\text{fb}^{-1}]$	Mass limit	Reference					
Inclusive Searches	$q\bar{q}, \tilde{q} \rightarrow q\tilde{\chi}_1^0$	0 e, μ mono-jet	2-6 jets E_T^{miss}	139 139	\tilde{q} [1x, 8x Degen.] \tilde{q} [8x Degen.]	1.0 0.9	1.85	$m(\tilde{\chi}_1^0) < 400 \text{ GeV}$ $m(\tilde{q}) - m(\tilde{\chi}_1^0) = 5 \text{ GeV}$	2010.14293 2102.10874
	$\tilde{g}\tilde{g}, \tilde{g} \rightarrow q\tilde{q}\tilde{\chi}_1^0$	0 e, μ	2-6 jets E_T^{miss}	139	\tilde{g}	Forbiddn	2.3	$m(\tilde{\chi}_1^0) = 0 \text{ GeV}$ $m(\tilde{g}) = 1000 \text{ GeV}$	2010.14293 2010.14293
	$\tilde{g}\tilde{g}, \tilde{g} \rightarrow q\tilde{q}W\tilde{\chi}_1^0$	1 e, μ	2-6 jets	139	\tilde{g}		2.2	$m(\tilde{\chi}_1^0) < 600 \text{ GeV}$	2101.01629
	$\tilde{g}\tilde{g}, \tilde{g} \rightarrow q\tilde{q}(\ell\ell)\tilde{\chi}_1^0$	e, μ, μ	2 jets E_T^{miss}	139	\tilde{g}		2.2	$m(\tilde{\chi}_1^0) < 700 \text{ GeV}$	2204.13072
	$\tilde{g}\tilde{g}, \tilde{g} \rightarrow q\tilde{q}WZ\tilde{\chi}_1^0$	0 e, μ	7-11 jets E_T^{miss}	139	\tilde{g}		1.97	$m(\tilde{\chi}_1^0) < 600 \text{ GeV}$	2008.06032
	$\tilde{g}\tilde{g}, \tilde{g} \rightarrow q\tilde{q}WZ\tilde{\chi}_1^0$	SS e, μ	6 jets	139	\tilde{g}		1.15	$m(\tilde{g}) - m(\tilde{\chi}_1^0) = 200 \text{ GeV}$	1909.08457
	$\tilde{g}\tilde{g}, \tilde{g} \rightarrow t\tilde{t}\tilde{\chi}_1^0$	0-1 e, μ SS e, μ	3 b 6 jets E_T^{miss}	139 139	\tilde{g} \tilde{g}		2.45 1.25	$m(\tilde{\chi}_1^0) < 500 \text{ GeV}$ $m(\tilde{g}) - m(\tilde{\chi}_1^0) = 300 \text{ GeV}$	2211.08028 1909.08457
	3 rd gen. squarks direct production	$\tilde{b}_1\tilde{b}_1$	0 e, μ	2 b E_T^{miss}	139	\tilde{b}_1 \tilde{b}_1		1.255 0.68	$m(\tilde{\chi}_1^0) < 400 \text{ GeV}$ $10 \text{ GeV} < \Delta m(\tilde{b}_1, \tilde{\chi}_1^0) < 20 \text{ GeV}$
$\tilde{b}_1\tilde{b}_1, \tilde{b}_1 \rightarrow b\tilde{\chi}_2^0 \rightarrow b\tilde{h}\tilde{\chi}_1^0$		0 e, μ 2 τ	6 b 2 τ E_T^{miss}	139 139	\tilde{b}_1 \tilde{b}_1	Forbiddn	0.23-1.35	$\Delta m(\tilde{\chi}_2^0, \tilde{\chi}_1^0) = 130 \text{ GeV}, m(\tilde{\chi}_1^0) = 100 \text{ GeV}$ $\Delta m(\tilde{\chi}_2^0, \tilde{\chi}_1^0) = 130 \text{ GeV}, m(\tilde{\chi}_1^0) = 0 \text{ GeV}$	1908.03122 2103.08189
$\tilde{t}_1\tilde{t}_1, \tilde{t}_1 \rightarrow t\tilde{\chi}_1^0$		0-1 e, μ	≥ 1 jet E_T^{miss}	139	\tilde{t}_1		1.25	$m(\tilde{\chi}_1^0) = 1 \text{ GeV}$	2004.14060, 2012.03799
$\tilde{t}_1\tilde{t}_1, \tilde{t}_1 \rightarrow Wb\tilde{\chi}_1^0$		1 e, μ	3 jets/1 b E_T^{miss}	139	\tilde{t}_1	Forbiddn	0.65	$m(\tilde{\chi}_1^0) = 500 \text{ GeV}$	2012.03799
$\tilde{t}_1\tilde{t}_1, \tilde{t}_1 \rightarrow \tilde{\tau}_1 b\nu, \tilde{\tau}_1 \rightarrow \tau\tilde{G}$		1-2 τ	2 jets/1 b E_T^{miss}	139	\tilde{t}_1	Forbiddn	1.4	$m(\tilde{\tau}_1) = 800 \text{ GeV}$	2108.07665
$\tilde{t}_1\tilde{t}_1, \tilde{t}_1 \rightarrow c\tilde{\chi}_1^0 / \tilde{c}\tilde{c}, \tilde{c} \rightarrow c\tilde{\chi}_1^0$		0 e, μ 2 c mono-jet E_T^{miss}	36.1 139	\tilde{t}_1 \tilde{t}_1			0.85 0.55	$m(\tilde{\chi}_1^0) = 0 \text{ GeV}$ $m(\tilde{t}_1, \tilde{c}) - m(\tilde{\chi}_1^0) = 5 \text{ GeV}$	1805.01649 2102.10874
$\tilde{t}_1\tilde{t}_1, \tilde{t}_1 \rightarrow t\tilde{\chi}_2^0, \tilde{\chi}_2^0 \rightarrow Z/h\tilde{\chi}_1^0$		1-2 e, μ	1-4 b E_T^{miss}	139	\tilde{t}_1		0.067-1.18	$m(\tilde{\chi}_2^0) = 500 \text{ GeV}$	2006.05880
$\tilde{b}_2\tilde{b}_2, \tilde{b}_2 \rightarrow \tilde{t}_1 + Z$		3 e, μ	1 b E_T^{miss}	139	\tilde{b}_2	Forbiddn	0.86	$m(\tilde{\chi}_1^0) = 360 \text{ GeV}, m(\tilde{t}_1) - m(\tilde{\chi}_1^0) = 40 \text{ GeV}$	2006.05880
RPV	$\tilde{\chi}_1^+ \tilde{\chi}_1^- / \tilde{\chi}_1^0, \tilde{\chi}_1^+ \rightarrow Z\ell\ell$	3 e, μ	0 jets E_T^{miss}	139	$\tilde{\chi}_1^+ / \tilde{\chi}_1^-$ [BR(Z τ)=1, BR(Z e)=1]	0.625	1.05	Pure Wino	2011.10543
	$\tilde{\chi}_1^+ \tilde{\chi}_1^- / \tilde{\chi}_2^0 \rightarrow W\nu/Z\ell\ell\nu\nu$	4 e, μ	0 jets	139	$\tilde{\chi}_1^+ / \tilde{\chi}_1^-$ [$A_{133} \neq 0, A_{124} \neq 0$]	0.95	1.55	$m(\tilde{\chi}_1^0) = 200 \text{ GeV}$	2103.11684 1804.03568
	$\tilde{g}\tilde{g}, \tilde{g} \rightarrow q\tilde{q}\tilde{\chi}_1^0, \tilde{\chi}_1^0 \rightarrow qq$	Multiple	4-5 large jets	36.1	\tilde{g} [$m(\tilde{\chi}_1^0) = 200 \text{ GeV}, 1100 \text{ GeV}$]	0.55	1.3	Large A'_{12}	ATLAS-CONF-2018-003
	$\tilde{t}\tilde{t}, \tilde{t} \rightarrow t\tilde{\chi}_1^0, \tilde{\chi}_1^0 \rightarrow tbs$	$\geq 4b$	Multiple	139	\tilde{t} [$A'_{33} = 2e-4, 1e-2$]	0.55	1.05	$m(\tilde{\chi}_1^0) = 200 \text{ GeV}$, bino-like	2010.01015
	$\tilde{t}\tilde{t}, \tilde{t} \rightarrow b\tilde{\chi}_1^0, \tilde{\chi}_1^0 \rightarrow bbs$	$\geq 4b$	Multiple	139	\tilde{t}	Forbiddn	0.95	$m(\tilde{\chi}_1^0) = 500 \text{ GeV}$	1710.07171
	$\tilde{t}_1\tilde{t}_1, \tilde{t}_1 \rightarrow bs$	2 jets + 2 b	Multiple	36.7	\tilde{t}_1 [qq, bs]	0.42	0.61		1710.05544
$\tilde{t}_1\tilde{t}_1, \tilde{t}_1 \rightarrow q\ell$	2 e, μ 1 μ	2 b DV	36.1 136	\tilde{t}_1		1.0	BR($\tilde{t}_1 \rightarrow b\ell$) > 20% BR($\tilde{t}_1 \rightarrow q\mu$) = 100%, $\cos\theta = 1$	2003.11956	
$\tilde{\chi}_1^+ \tilde{\chi}_1^- / \tilde{\chi}_1^0, \tilde{\chi}_1^0 \rightarrow tbs, \tilde{\chi}_1^+ \rightarrow bbs$	1-2 e, μ	≥ 6 jets	139	$\tilde{\chi}_1^+$		0.2-0.32	Pure higgsino	2106.09609	

*Only a selection of the available mass limits on new states or phenomena is shown. Many of the limits are based on simplified models, c.f. refs. for the assumptions made.

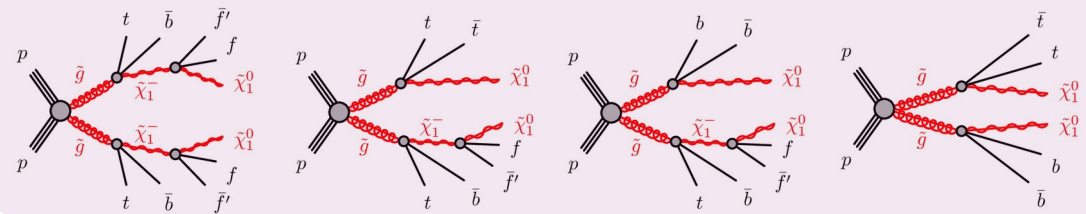
All ATLAS SUSY results [here](#)

- Multiple SRs targeting pair production of gluinos decaying, directly or via the lightest chargino, to top and/or bottom quarks and the lightest neutralino.

Gtt and Gbb models with 100% gluino BR to specific final state



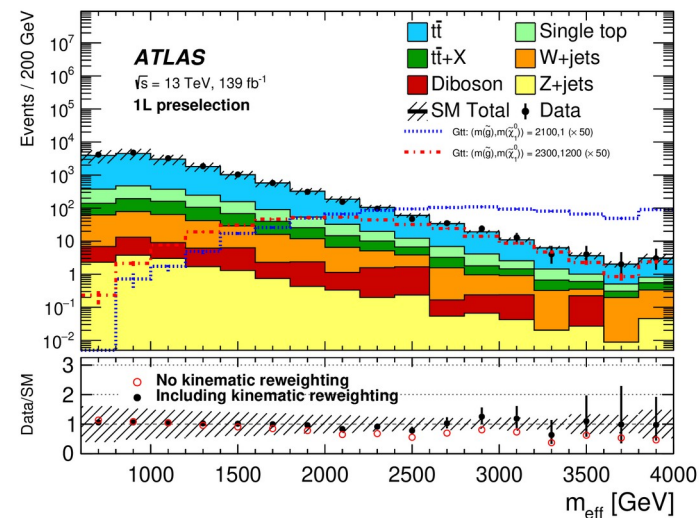
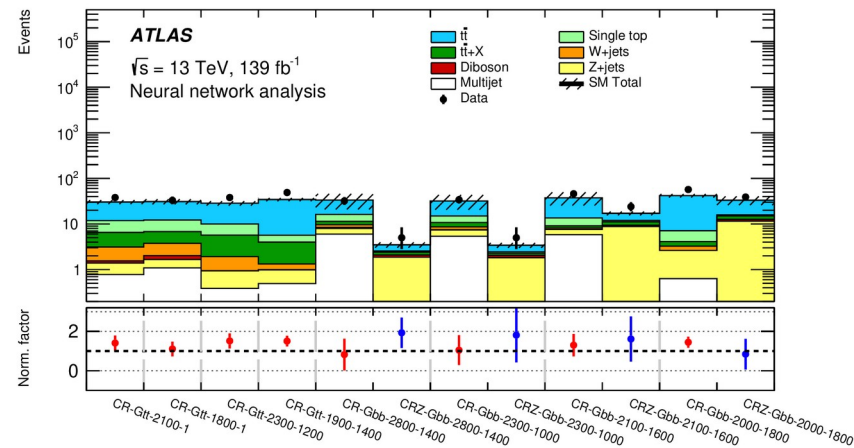
Gtb models with variable gluino BR, and chargino-neutralino mass difference of 2 GeV



- Exploits both cut-and-count (CC) and neural network (NN) SRs.
- All SRs require large E_{τ}^{miss} ; at least three b-tagged jets; exactly zero (0L) or at least one (1L) charged lepton.
- NN trained to discriminate Gtt and Gbb signals from the SM background using p_{τ}^{miss} vector and 4-momenta of jets and leptons as input.
- NN classifies events as Gtt/Gbb, $t\bar{t}$ or Z+jets.

Glino production in multi-b final states

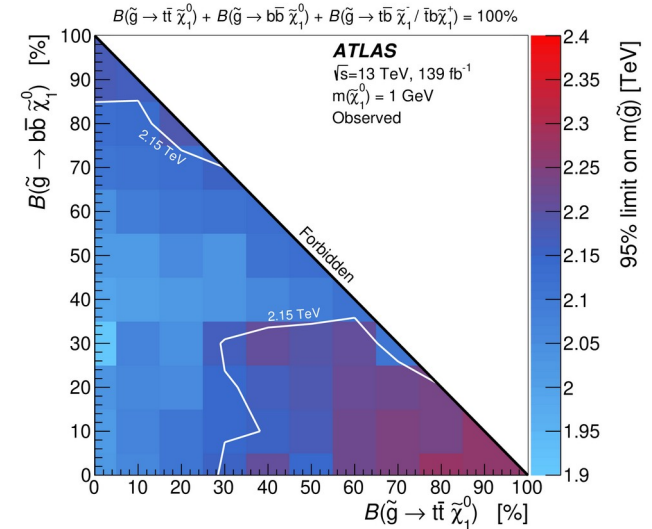
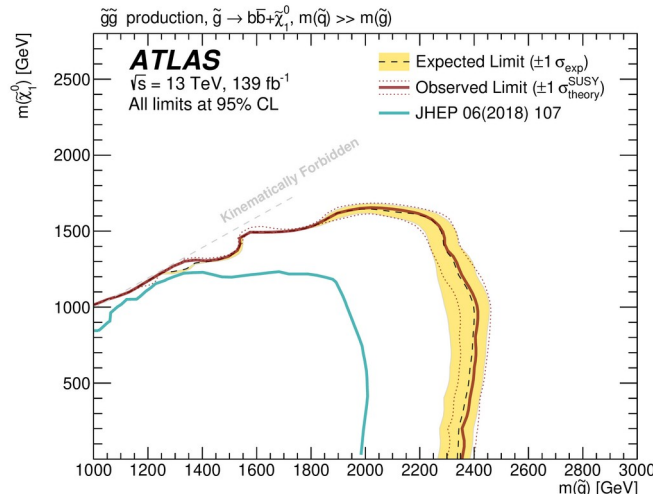
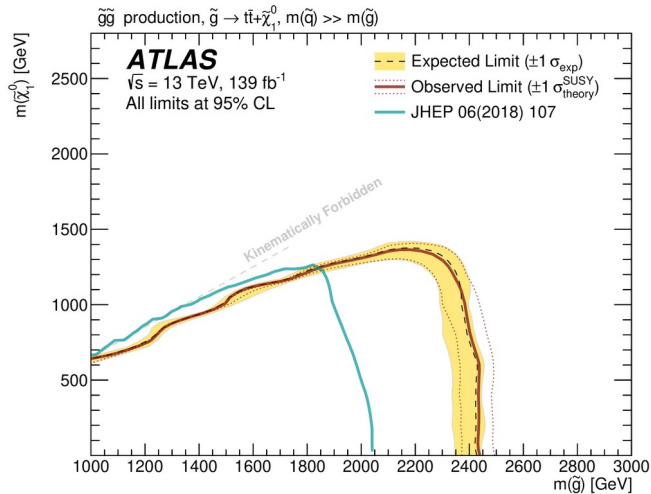
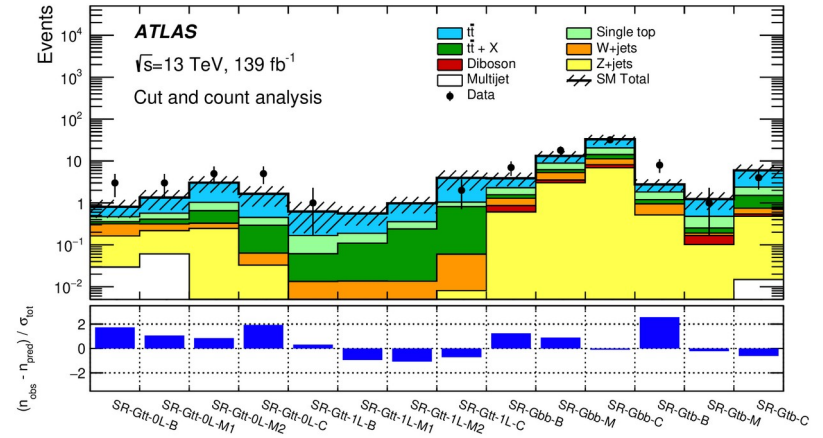
- Dominant backgrounds
 - $t\bar{t}$ (all channels) and Z+jets (Gbb NN only)
 - Estimated using CRs, built from NN scores and/or variables such as $m_{\text{eff}} = \text{sum}(p_T^{\text{jet}}) + \text{sum}(p_T^{\text{lept}}) + E_T^{\text{miss}}$, m_T , and $M_J^Z = \text{sum of large-R jet masses}$.
 - Background normalization factors from CRs are close to or consistent with unity in all cases.
- Minor backgrounds
 - single top, W+jets, Z+jets, $t\bar{t}+X$, $t\bar{t}\bar{t}$, diboson
 - Estimated from simulated events.
- Multi-jet background
 - Data-driven estimate using dedicated CR.
- 1L regions suffer from a p_T -related mismodelling visible in e.g. m_{eff} and E_T^{miss} (not there in 0L regions).
- Kinematic reweighting of m_{eff} spectrum derived in data in dedicated reweighting regions and applied to MC.



Gluino production in multi-b final states

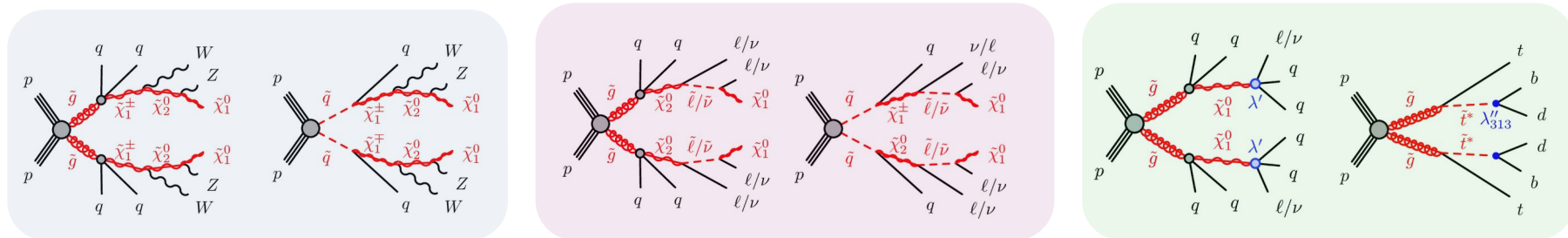
6

- No significant excess over the SM background prediction is observed in any SR. → Set mass limits.
- Gluino masses below 2.44 and 2.35 TeV are excluded at 95% CL for massless neutralinos in Gtt and Gbb models, respectively.
- Exclusions in the Gtb models are presented as a function of branching ratios $\tilde{g} \rightarrow tt$ and $\tilde{g} \rightarrow bb$.
- Strongest limits when a single decay ($\tilde{g} \rightarrow tt$ or $\tilde{g} \rightarrow bb$) dominates, and weaker when the two BRs are more similar.



Glino and squark production in multi-lepton final states

- Large set of SRs targeting gluino and squark production with subsequent cascade decays involving **charginos and neutralinos**, **intermediate sleptons**, **R-parity violating couplings**.

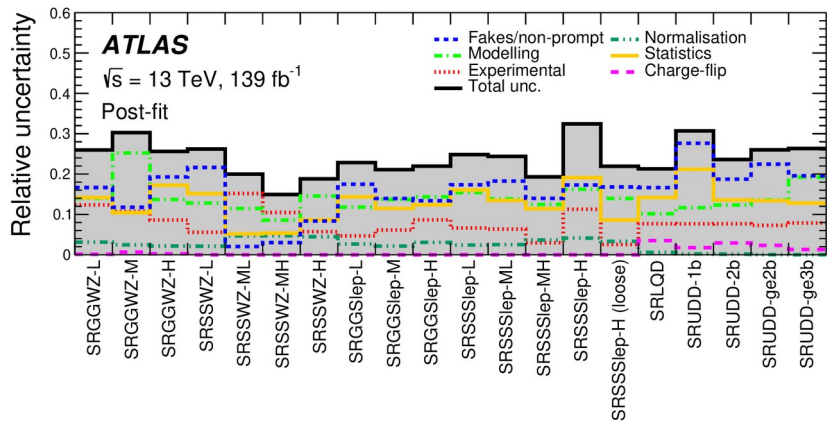


- Masses of intermediate superpartners are half way between \tilde{g}/\tilde{q} and lightest neutralino.
- Separate SRs targeting low, medium and large \tilde{g}/\tilde{q} - neutralino mass splittings.
- Final states include either two charged leptons with the same electric charge (SS) or at least three charged leptons (3L).
- Additional requirements placed e.g. on E_T^{miss} , number of (b-tagged) jets, Σp_T^{jet} and m_{eff} .

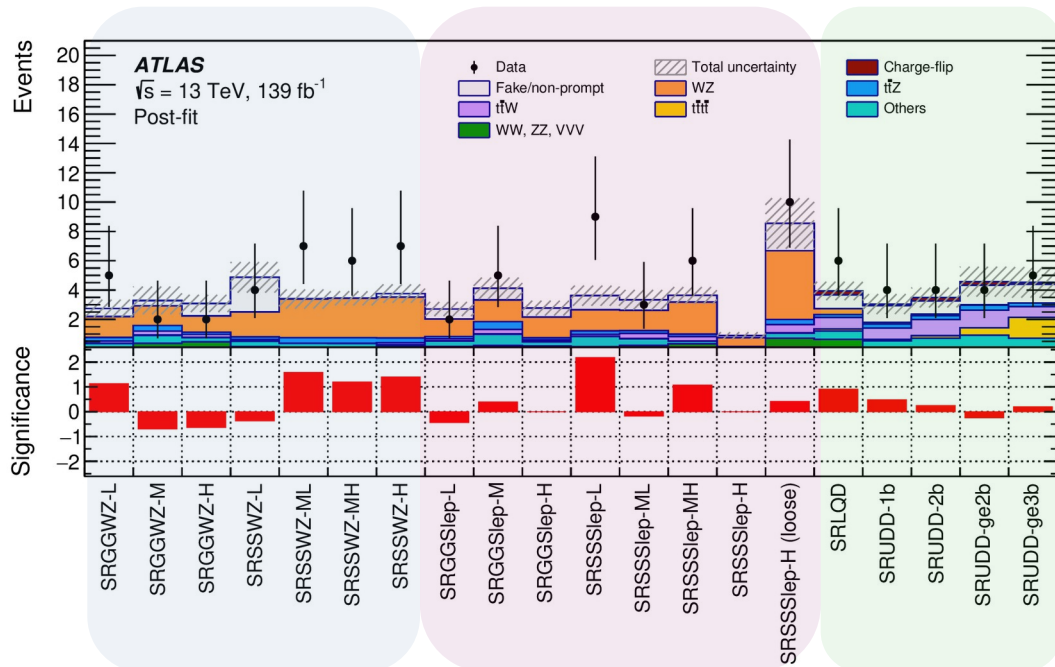
Glino and squark production in multi-lepton final states

SUSY-2020-27

- WZ+jets background is estimated using a CR in data.
- Backgrounds containing electrons with incorrect charge are estimated directly in data.
- Backgrounds with fake or non-prompt leptons are estimated in data using a matrix method.
- $t\bar{t}V$, $t\bar{t}t$, $WW/ZZ/VV$, $t\bar{t}+X$, single top and tW are all estimated with simulated events.
- Systematic uncertainties related to estimation of fake/non-prompt leptons dominate.



- No significant excess over the SM background prediction is observed.
 → set mass limits.

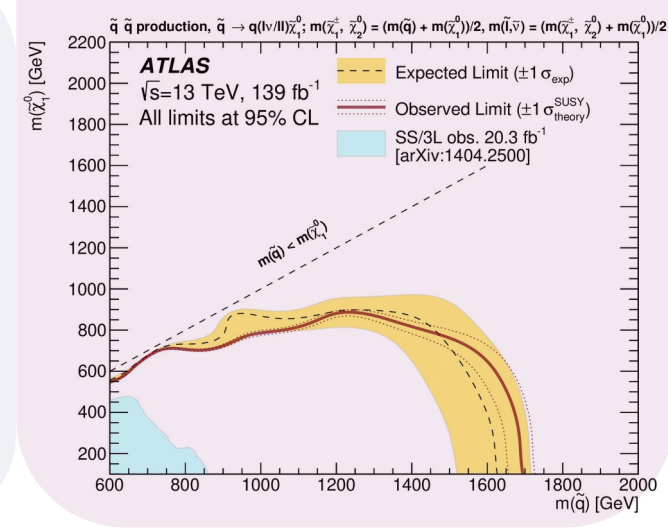
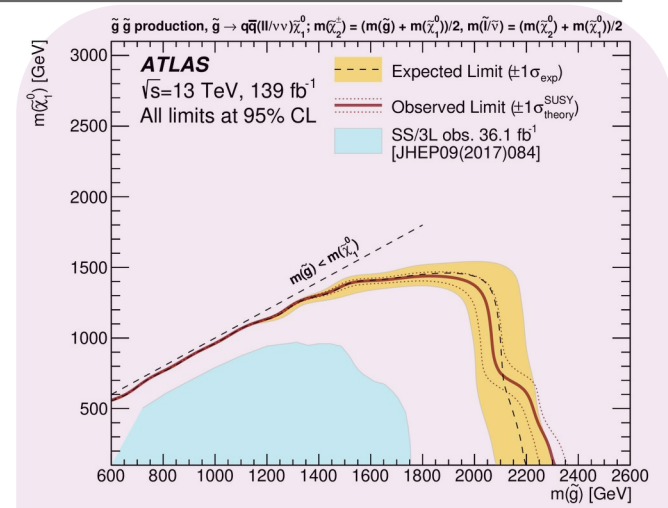
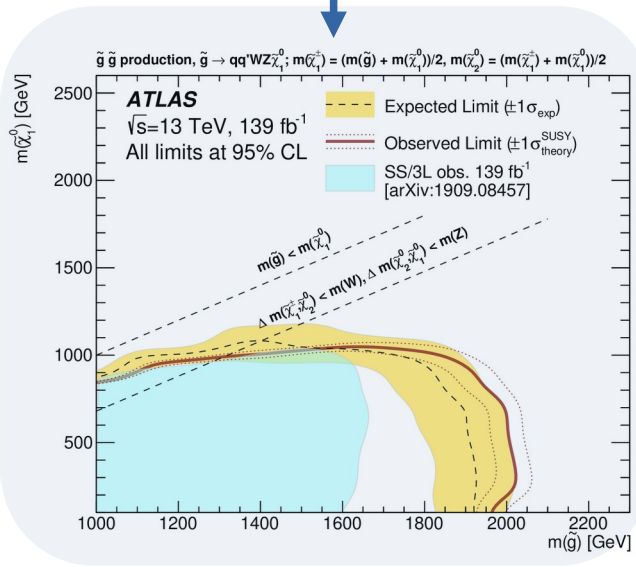
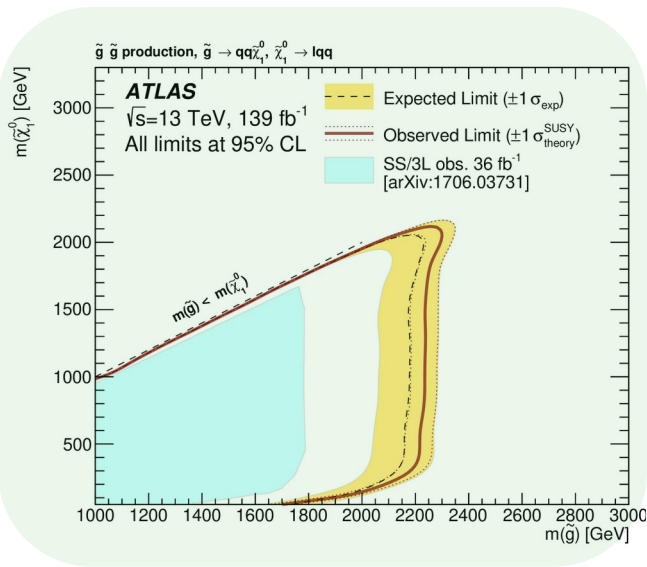


Glino and squark production in multi-lepton final states

- Gluino masses up to maximum 2.2 TeV are excluded, in RPC as well as RPV scenarios.
- Squark masses are excluded up to maximum 1.7 TeV.

 SUSY-2020-27

Significant improvement with respect to previous analysis on the same dataset, thanks to improved analysis techniques and the inclusion of a CR for the WZ+jets background.

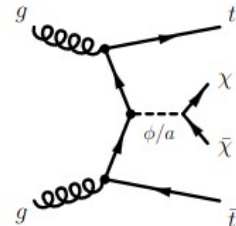
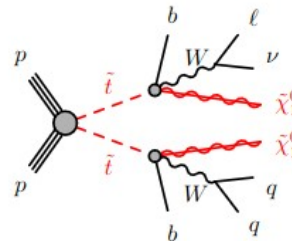
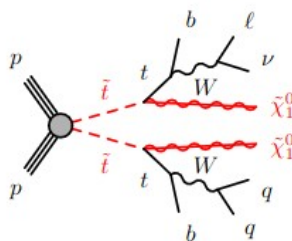


Stop production in $t\bar{t}+E_T^{\text{miss}}$ final states



See poster by Simran Gurdasani

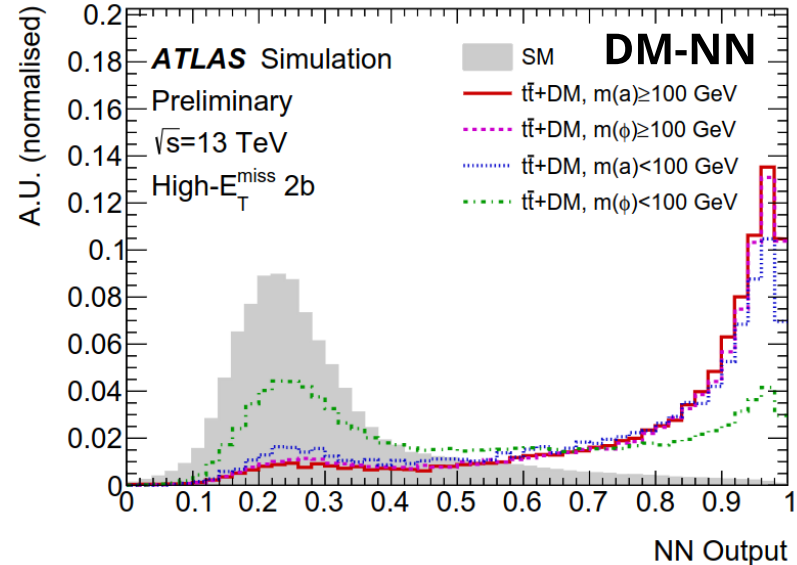
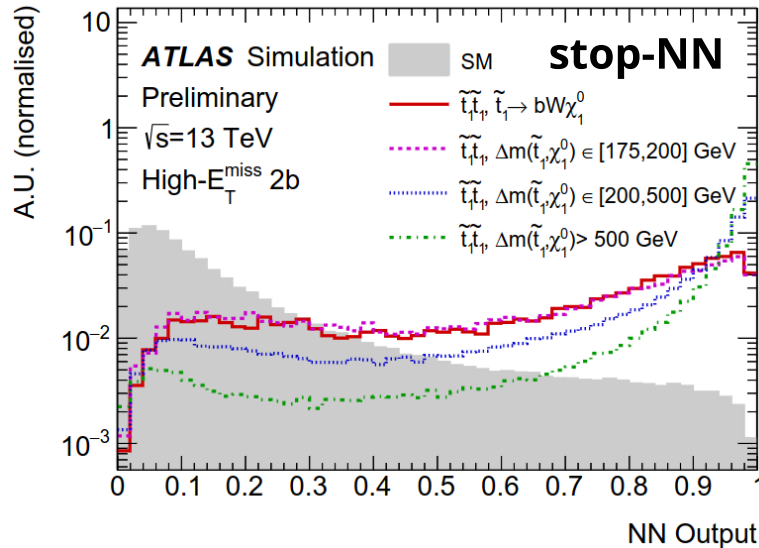
- Search targets direct stop production as well as $t\bar{t}$ +DM models.
- Novel analysis technique that provides sensitivity over a wide range of the parameter space.
- In particular, the sensitivity to models with a stop-neutralino mass splitting around the top mass is greatly improved.
- Events are required to have exactly one charged and isolated lepton.
- They are further split into eight orthogonal categories based on:
 - the E_T^{miss} (high- E_T^{miss} or boosted);
 - the number of b-tagged jets (1 or 2);
 - the presence of top-tagged large-radius jets (0 or 1).
- The major backgrounds - $t\bar{t}$, single top and W+jets - are estimated using CRs in data.
- Minor backgrounds are estimated directly from simulated events.
- The irreducible $t\bar{t}Z$ background is validated in a dedicated $t\bar{t}Z(\rightarrow ll)$ VR.



Category

High- E_T^{miss} 1b
High- E_T^{miss} 2b
Boosted 1b-lep-1t
Boosted 1b-had-1t
Boosted 2b-1t
Boosted 1b-lep-0t
Boosted 1b-had-0t
Boosted 2b-0t

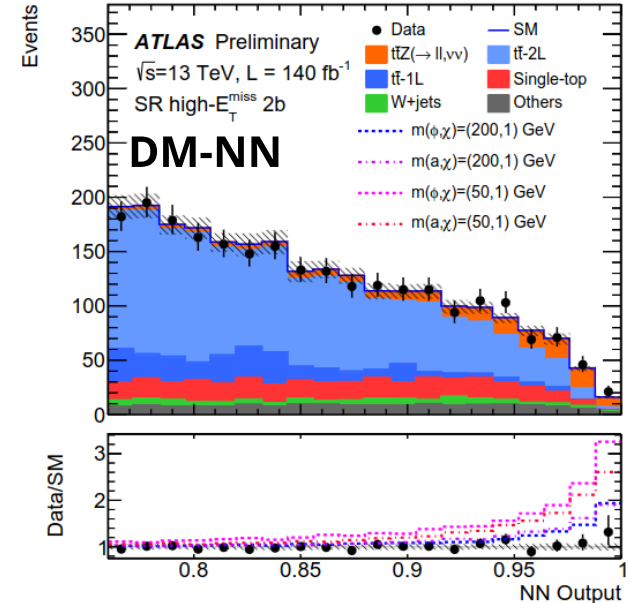
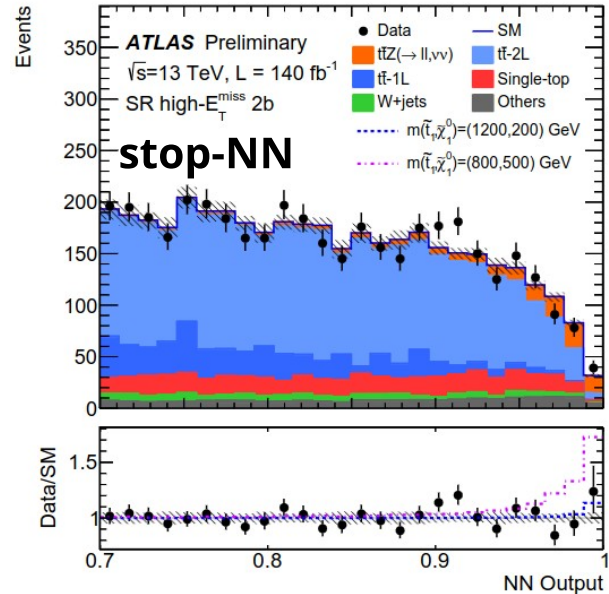
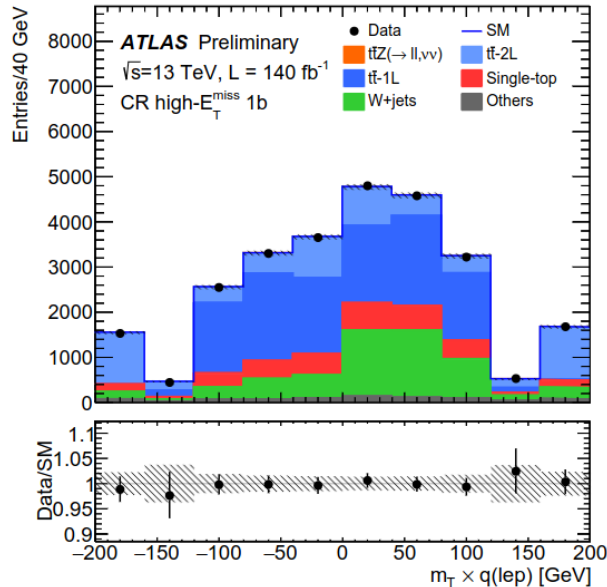
- In each category, dedicated NNs are trained to separate the signal from the SM background.
 - High- E_T^{miss} : Both stop and $t\bar{t}$ +DM signals targeted with two different NNs.
 - Boosted: Only stop signal targeted.
- The NNs are trained with signal χ events from all mass points in the parameter space.
- Binned fit to the NN score distribution is used to gain sensitivity to all signals.



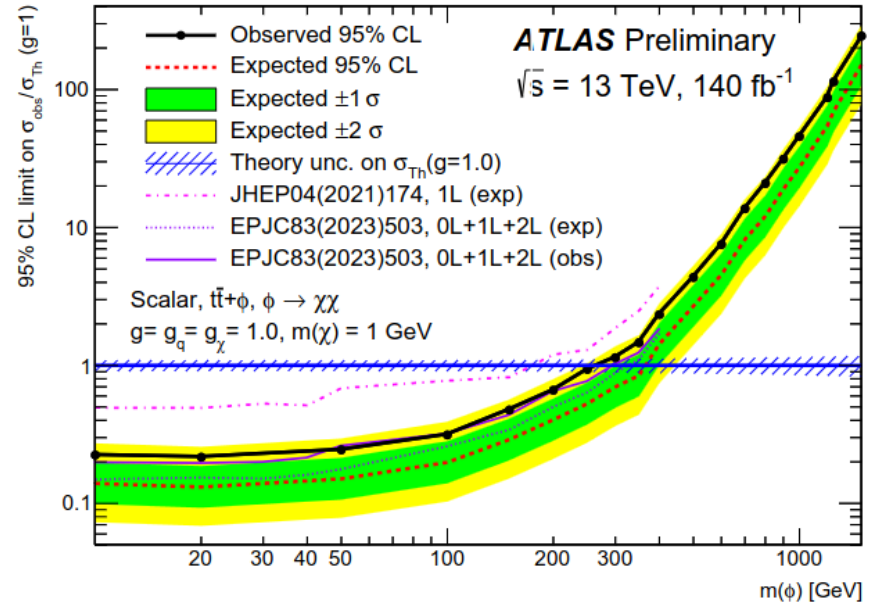
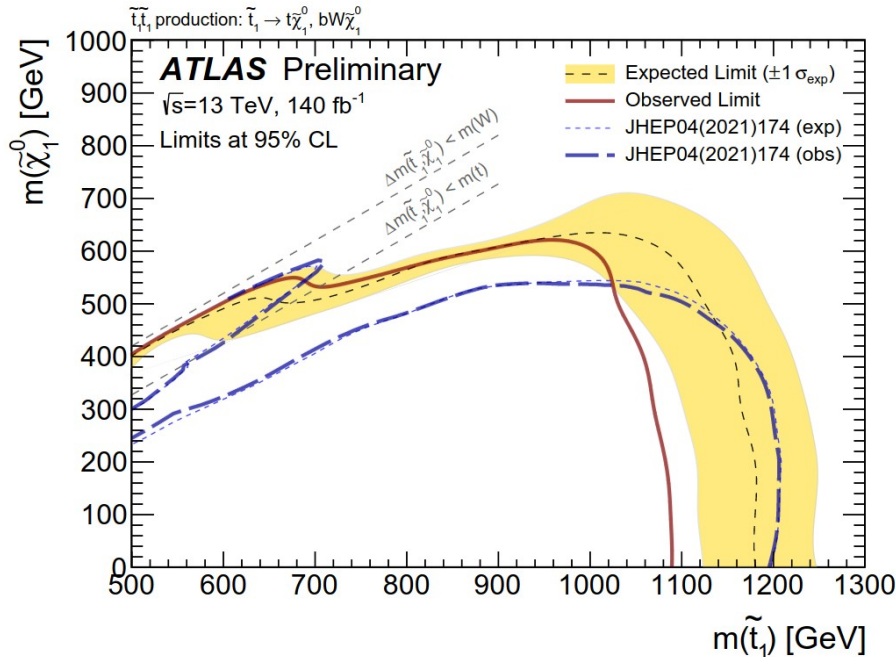
- Each event category split into SR, CR and VR based on stop-NN and DM-NN output scores.

Stop production in $t\bar{t}+E_T^{\text{miss}}$ final states

- The $t\bar{t}$, single top and W+jets background normalization factors are all compatible with unity.
- Significantly improved background modelling compared to the previous result thanks to:
 - the simulation of the $t\bar{t}$ production with Sherpa;
 - the simulation of the tW production with dynamic scales.
- No significant excess over the SM background is observed in any of the SRs \rightarrow set mass limits.

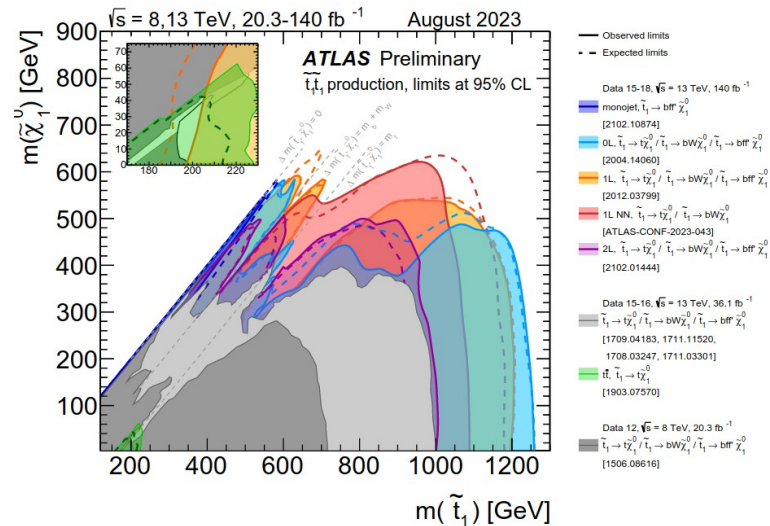
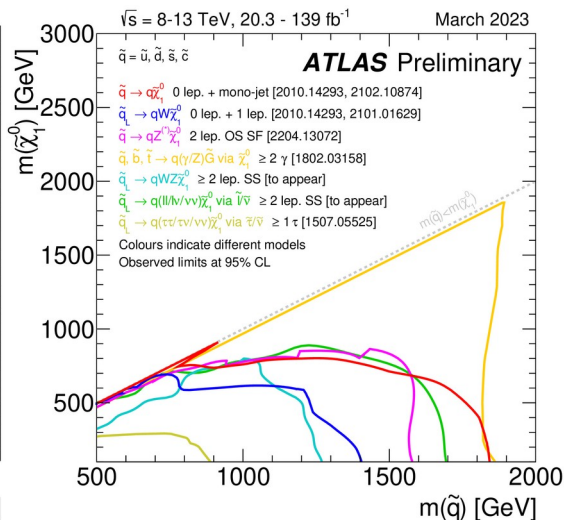
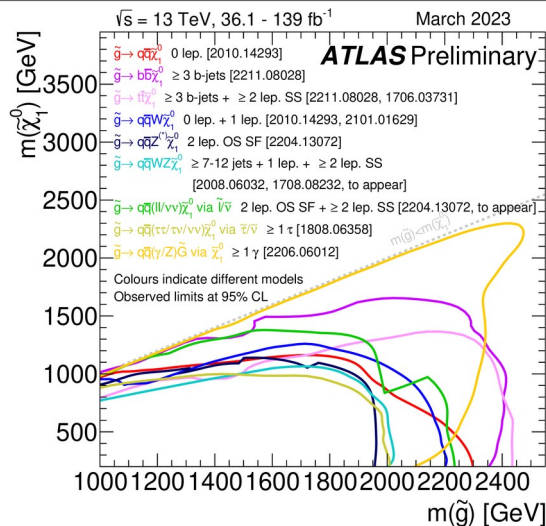


- At small neutralino masses, stop masses up to 1090 GeV are excluded at 95% CL.
 - The weaker observed limits at high stop mass are due to a small excess of data in the bins at highest NN score in the high- E_T^{miss} and boosted 2b SRs.
- Scalar (pseudoscalar) dark matter mediator masses up to 250 (300) GeV are excluded for a mediator coupling strength $g_{\text{DM}}=g_{\text{SM}}=1$.



Summary and outlook

- Many final Run-2 results becoming available (three shown in this talk).
- Also start to see the first Run-3 results.
- No evidence for SUSY yet.
- In most favourable scenarios we exclude
 - gluinos up to O(2.5) TeV
 - squarks up to O(1.8) TeV
 - stops and sbottoms up to O(1.2) TeV
- But large regions of parameter space are still unconstrained.
- Run 3 and beyond will bring sensitivity to difficult regions of parameter space that are still not well covered.
- Next step is to complete the program with the full Run-3 dataset.



Backup material

Gluino production in multi-b final states

Table 1: List of MC generators used to simulate different signal and background processes. The third column (“Tune”) describes the tuned set of underlying event and hadronisation parameters, the fourth column the PDF set used, and the fifth column the perturbative accuracy in the strong coupling constant used for the calculation of the cross-section used to normalise the sample.

Process	Generator + fragmentation/hadronisation	Tune	PDF set	Cross-section order
Gbb/Gtb/Gtt	MADGRAPH5_AMC@NLO 2.2.2 [37] + PYTHIA 8.186	A14 [38]	NNPDF2.3 [39]	NLO+NLL [40–45]
$t\bar{t}$	POWHEG BOX v2 + PYTHIA 8.230	A14	NNPDF3.0	NNLO+NNLL [46]
Single top <i>s/t</i> -channel	POWHEG BOX v2 + PYTHIA 8.230	A14	NNPDF3.0	NLO [47, 48]
Single top W_t	POWHEG BOX v2 + PYTHIA 8.230	A14	NNPDF3.0	approx. NNLO [49, 50]
$t\bar{t}W/t\bar{t}Z$	MADGRAPH5_AMC@NLO 2.3.3 + PYTHIA 8.230	A14	NNPDF3.0	NLO [37]
$t\bar{t}\bar{t}$	MADGRAPH 2.3.3 + PYTHIA 8.230	A14	NNPDF2.3	NLO [37]
$t\bar{t}H$	POWHEG BOX v2 + PYTHIA 8.230	A14	NNPDF2.3	NLO [37]
Diboson WW, WZ, ZZ	SHERPA 2.2.1 [51]	Default	NNPDF3.0	NLO [51, 52]
W/Z+jets	SHERPA 2.2.1	Default	NNPDF3.0	NNLO [53]

Gluino production in multi-b final states

17

Table 2: Definitions of the reweighting regions used to derive the m_{eff} reweighting factors applied to the MC samples. The N_{lepton} requirements apply to signal leptons. The Z and VV RR uses a definition of $E_{\text{T}}^{\text{miss}}$ ($\hat{E}_{\text{T}}^{\text{miss}}$) that adds the lepton pair's transverse momentum to the missing transverse momentum, to simulate $Z \rightarrow \nu\nu$ events.

Criteria common to all regions: $N_{\text{jet}} \geq 4$, $E_{\text{T}}^{\text{miss}}$ or $\hat{E}_{\text{T}}^{\text{miss}} \geq 200$ GeV				
Reweighting Region	N_{lepton}	$N_{b\text{-jets}}$	$m_{\text{T,min}}^{b\text{-jets}}$ [GeV]	$m_{\ell\ell}$ [GeV]
$t\bar{t}$	= 1	= 2	≤ 350	-
Single top, $t\bar{t} + W/Z/H$, $t\bar{t}t\bar{t}$	= 1	= 2	> 350	-
W +jets	= 1	= 0	-	-
Z +jets, VV	= 2 opposite charge	= 0	-	$\in [60, 120]$

- RRs are orthogonal to all analysis signal regions, which include a $N_{b\text{-jets}} \geq 3$ requirement.
- Data/MC (after MC normalized to data) ratio derived vs m_{eff} in bins of N_{jet} .
- Ratios are fitted with a decreasing exponential, which is used to reweight MC.
- Reweighting factors range from 1.7 to 0.19.

Gluino production in multi-b final states

Table 3: Event selection requirements for the CC Gtt 0-lepton SRs together with the associated $t\bar{t}$ CRs and VRs, classified according to the $\tilde{g}-\tilde{\chi}_1^0$ mass splitting (Δm) targeted. The thresholds in bold for each control and validation region ensure orthogonality with the corresponding signal region. $N_{\text{lepton}} = 0$ requires zero baseline leptons, while $N_{\text{lepton}} = 1$ requires one signal lepton.

Targeted kinematics	Type	N_{lepton}	N_{jet}	$N_{b\text{-jets}}$	$E_{\text{T}}^{\text{miss}}$ [GeV]	$\Delta\phi_{\text{min}}^{4j}$	m_{eff} [GeV]	m_{T} [GeV]	$m_{\text{T,min}}^{b\text{-jets}}$ [GeV]	M_{J}^{Σ} [GeV]
Region B (Boosted, Large Δm)	SR	= 0	≥ 5	≥ 3	≥ 600	≥ 0.4	≥ 2900	–	≥ 120	≥ 300
	CR	= 1	≥ 4	≥ 3	≥ 200	–	≥ 2000	< 150	–	≥ 150
	VR	= 0	≥ 5	≥ 3	≥ 250	≥ 0.4	≥ 2000	–	–	< 300
Region M1 (Moderate Δm)	SR	= 0	≥ 9	≥ 3	≥ 600	≥ 0.4	≥ 1700	–	≥ 120	≥ 300
	CR	= 1	≥ 8	≥ 3	≥ 200	–	≥ 1100	< 150	–	≥ 150
	VR	= 0	≥ 9	≥ 3	≥ 300	≥ 0.4	≥ 1400	–	–	< 300
Region M2 (Moderate Δm)	SR	= 0	≥ 10	≥ 3	≥ 500	≥ 0.4	≥ 1100	–	≥ 120	≥ 200
	CR	= 1	≥ 9	≥ 3	≥ 200	–	≥ 800	< 150	–	≥ 100
	VR	= 0	≥ 10	≥ 3	≥ 300	≥ 0.4	≥ 800	–	–	< 200
Region C (Compressed, small Δm)	SR	= 0	≥ 10	≥ 4	≥ 400	≥ 0.4	≥ 800	–	≥ 180	≥ 100
	CR	= 1	≥ 9	≥ 4	≥ 200	–	≥ 800	< 150	–	≥ 100
	VR	= 0	≥ 10	≥ 4	≥ 200	≥ 0.4	≥ 800	–	–	< 100

Gluino production in multi-b final states

Table 4: Event selection requirements for the CC Gtt 1-lepton SRs together with the associated $t\bar{t}$ CRs and VRs, classified according to the $\tilde{g}-\tilde{\chi}_1^0$ mass splitting (Δm) targeted. The thresholds in bold for each control and validation region ensure orthogonality with the corresponding signal region.

Targeted kinematics	Type	N_{jet}	E_T^{miss} [GeV]	m_{eff} [GeV]	m_T [GeV]	$m_{T,\text{min}}^{b\text{-jets}}$ [GeV]	M_J^Σ [GeV]
Region B (Boosted, Large Δm)	SR	≥ 4	≥ 600	≥ 2300	≥ 150	≥ 120	≥ 200
	CR	$= 4$	≥ 200	≥ 1500	< 150	–	–
	VR1	≥ 4	≥ 200	≥ 1500	≥ 150	–	< 200
	VR2	≥ 5	≥ 200	≥ 1200	< 150	≥ 120	≥ 200
Region M1 (Moderate Δm)	SR	≥ 5	≥ 600	≥ 2000	≥ 200	≥ 120	≥ 200
	CR	$= 5$	≥ 200	≥ 1200	< 200	–	–
	VR1	≥ 5	≥ 200	≥ 1200	≥ 200	–	< 200
	VR2	≥ 6	≥ 200	≥ 1000	< 200	≥ 120	≥ 100
Region M2 (Moderate Δm)	SR	≥ 8	≥ 500	≥ 1100	≥ 200	≥ 120	≥ 100
	CR	$= 8$	≥ 200	≥ 800	< 200	–	–
	VR1	≥ 8	≥ 200	≥ 800	≥ 200	–	< 100
	VR2	≥ 9	≥ 200	≥ 800	< 200	≥ 120	≥ 100
Region C (Compressed, small Δm)	SR	≥ 9	≥ 300	≥ 800	≥ 150	≥ 120	–
	CR	$= 9$	≥ 200	≥ 800	< 150	–	–
	VR1	≥ 9	≥ 200	≥ 800	≥ 150	< 120	–
	VR2	≥ 10	≥ 200	≥ 800	< 150	≥ 120	–

Gluino production in multi-b final states

Table 5: Event selection requirements for the CC Gbb 0-lepton SRs together with the associated $t\bar{t}$ CRs and VRs, classified according to the $\tilde{g}-\tilde{\chi}_1^0$ mass splitting (Δm) targeted. The thresholds in bold for each control and validation region ensure orthogonality with the corresponding signal region. $N_{\text{lepton}} = 0$ requires zero baseline leptons, while $N_{\text{lepton}} = 1$ requires one signal lepton.

Targeted kinematics	Type	N_{lepton}	$p_{\text{T}}^{\text{jet}}$ [GeV]	m_{eff} [GeV]	$E_{\text{T}}^{\text{miss}}$ [GeV]	$m_{\text{T},\text{min}}^{b\text{-jets}}$ [GeV]	m_{T} [GeV]
Region B (Boosted, Large Δm)	SR	= 0	> 65	> 2600	> 550	> 130	
	CR	= 1	> 65	> 2600	> 450		< 150
	VR	= 0	> 65	< 2400	> 550	> 130	
Region M (Moderate Δm)	SR	= 0	> 30	> 2000	> 550	> 130	
	CR	= 1	> 30	> 2000	> 550		< 150
	VR	= 0	> 30	> 1600	< 500	> 80	
Region C (Compressed, small Δm)	SR	= 0	> 30	> 1600	> 550	> 130	
	CR	= 1	> 30	> 1600	> 550		< 150
	VR	= 0	> 30	> 1500	< 450	> 130	

Gluino production in multi-b final states

Table 6: Event selection requirements for the CC Gtb 0-lepton SRs together with the associated $t\bar{t}$ CRs and VRs, classified according to the $\tilde{g}-\tilde{\chi}_1^0$ mass splitting (Δm) targeted. The thresholds in bold for each control and validation region ensure orthogonality with the corresponding signal region. $N_{\text{lepton}} = 0$ requires zero baseline leptons, while $N_{\text{lepton}} = 1$ requires one signal lepton.

Targeted kinematics	Type	N_{lepton}	N_{jet}	$N_{b\text{-jets}}$	m_{eff} [GeV]	$E_{\text{T}}^{\text{miss}}$ [GeV]	$m_{\text{T,min}}^{b\text{-jets}}$ [GeV]	m_{T} [GeV]	M_{J}^{Σ} [GeV]
Region B (Boosted, Large Δm)	SR	= 0	≥ 4	≥ 3	> 2500	> 550	> 130		> 200
	CR	= 1	≥ 4	≥ 3	> 2200	> 400		< 150	> 200
	VR	= 0	≥ 4	≥ 3	< 2500	> 450	> 130		> 200
Region M (Moderate Δm)	SR	= 0	≥ 6	≥ 4	> 2000	> 550	> 130		> 200
	CR	= 1	≥ 6	≥ 4	> 1700	> 300		< 150	> 200
	VR	= 0	≥ 6	≥ 4	> 1600	< 550	> 110		> 200
Region C (Compressed, small Δm)	SR	= 0	≥ 7	≥ 4	> 1300	> 500	> 130		> 50
	CR	= 1	≥ 7	≥ 4	> 1300	> 350		< 150	> 50
	VR	= 0	≥ 7	≥ 4	> 1300	< 500	> 80		> 50

Gluino production in multi-b final states

22

- NN input variables:
 - The four-momenta (p_T , η , ϕ , m) of the 10 leading jets, in decreasing order of p_T , and a set of binary variables indicating which jets are b -tagged;
 - The four-momenta of the four leading large- R jets, in decreasing order of p_T ;
 - The four-momenta of the four leading leptons (e or μ), in decreasing order of p_T ;
 - The two components of the vector \vec{p}_T^{miss} .
- If a given event contains fewer jets or leptons, remaining inputs are set to zero.
- NN generates three output scores measuring the probability of a given event being a signal event ($P(\text{Gtt})$ or $P(\text{Gbb})$, depending on the signal model targeted), a tt background event ($P(tt)$), or a Z +jets background event ($P(Z)$).
- A parameterised training method used, where the NN was also given the gluino and neutralino mass pair of considered signal, as well as a binary variable indicating if discrimination of background versus Gtt or Gbb is required.
- Background events were assigned random parameter values.
- A set-cover algorithm was used to iteratively select the SR which excludes the most as-yet non-excluded model points, resulting in eight SRs expected to exclude the same number of Gtt or Gbb models as the one-SR-per-grid-point case.
 - **Gtt**: (2100, 1), (1800, 1), (2300, 1200), (1900, 1400)
 - **Gbb**: (2800, 1400), (2300, 1000), (2100, 1600), (2000, 1800)

Gluino production in multi-b final states

Table 7: Definitions of the NN Gtt SRs together with the associated $t\bar{t}$ CRs and VRs. In the first column, the two numbers separated by a hyphen specify the values of $m(\tilde{g})$ and $m(\tilde{\chi}_1^0)$ in GeV for the targeted representative Gtt model. The third and fourth columns specify the ranges of probability for the targeted Gtt signal model and $t\bar{t}$ background, respectively, generated by the selection applied to the NN output. The fifth and sixth columns specify the values of additional requirements applied to m_{eff} and M_J^Σ in the CRs and VRs to select events with kinematics similar to those in the corresponding SRs.

Representative model	Region	$P(\text{Gtt})$	$\log_{10}(P(t\bar{t}))$	m_{eff} [GeV]	M_J^Σ [GeV]
Gtt-2100-1	SR	≥ 0.9997	-	-	-
	CR	$\in (0.68, 0.86)$	≥ -1.8	≥ 2000	-
	VR	$\in (0.86, 0.9997)$	-	≥ 2000	-
Gtt-1800-1	SR	≥ 0.9997	-	-	-
	CR	$\in (0.73, 0.89)$	≥ -2.0	≥ 2000	-
	VR	$\in (0.89, 0.9997)$	-	≥ 2000	-
Gtt-2300-1200	SR	≥ 0.9993	-	-	-
	CR	$\in (0.78, 0.83)$	≥ -1.6	≥ 1400	-
	VR	$\in (0.83, 0.9993)$	-	≥ 1800	-
Gtt-1900-1400	SR	≥ 0.9987	-	-	-
	CR	$\in (0.78, 0.8)$	≥ -1.4	≥ 800	< 700
	VR	$\in (0.8, 0.9987)$	-	≥ 800	< 700

Gluino production in multi-b final states

Table 8: Definitions of the NN Gbb SRs together with the associated $t\bar{t}$ CRs and VRs. In the first column, the two numbers separated by a hyphen specify the values of $m(\tilde{g})$ and $m(\tilde{\chi}_1^0)$ in GeV for the targeted representative Gbb model. The third, fourth and fifth columns specify the ranges of probability for the targeted Gbb signal model and the $t\bar{t}$ or Z +jets background, respectively, generated by the selection applied to the NN output. The sixth, seventh and eighth columns specify the values of additional requirements applied to $\Delta\phi_{\min}^{4j}$, m_{eff} and M_J^Σ in the CRs and VRs to select events with kinematics similar to those in the corresponding SRs.

Rep. model	Region	$P(\text{Gbb})$	$\log_{10}(P(t\bar{t}))$	$\log_{10}(P(Z))$	$\Delta\phi_{\min}^{4j}$	m_{eff} [GeV]	M_J^Σ [GeV]
Gbb-2800-1400	SR	≥ 0.999	-	-	≥ 0.6	-	-
	CR	$\in (0.43, 0.76)$	≥ -0.7	-	≥ 0.5	≥ 1400	< 800
	VR1	$\in (0.76, 0.999)$	-	< -1.7	≥ 0.5	≥ 2500	< 800
	VR2	$\in (0.76, 0.999)$	-	≥ -1.7	≥ 0.5	-	-
Gbb-2300-1000	SR	≥ 0.9994	-	-	≥ 0.6	-	-
	CR	$\in (0.52, 0.77)$	≥ -0.8	-	≥ 0.5	≥ 1400	< 800
	VR1	$\in (0.77, 0.9994)$	-	< -1.3	≥ 0.5	≥ 2400	< 800
	VR2	$\in (0.77, 0.9994)$	-	≥ -1.3	≥ 0.5	-	-
Gbb-2100-1600	SR	≥ 0.9993	-	-	≥ 0.4	-	-
	CR	$\in (0.88, 0.91)$	≥ -1.3	-	≥ 0.4	≥ 800	< 500
	VR1	$\in (0.91, 0.9993)$	-	< -1.4	≥ 0.4	≥ 800	< 500
	VR2	$\in (0.91, 0.9993)$	-	≥ -1.4	≥ 0.4	-	-
Gbb-2000-1800	SR	≥ 0.997	-	-	≥ 0.4	-	-
	CR	$\in (0.92, 0.93)$	≥ -1.9	-	≥ 0.4	≥ 400	< 400
	VR1	$\in (0.93, 0.997)$	-	< -1.4	≥ 0.4	≥ 400	< 400
	VR2	$\in (0.93, 0.997)$	-	≥ -1.4	≥ 0.4	-	-

Gluino production in multi-b final states

25

Table 9: Definitions of the NN Gbb Z+jets CRs (CRZ). The first seven rows specify the event selection criteria. The final three rows specify the ranges of probability for the targeted Gbb signal model and the $t\bar{t}$ or Z+jets background, respectively, generated by the selection applied to the NN output. $N_{\text{lepton}} = 2$ requires two signal leptons.

	Gbb-2800-1400	Gbb-2300-1000	Gbb-2100-1600	Gbb-2000-1800
$N_{\text{lepton}} (p_T(\ell) > 30 \text{ GeV})$			= 2	
$m_{\ell(1),\ell(2)} [\text{GeV}]$			$\in [60, 120]$	
$p_T(\ell(1), \ell(2)) [\text{GeV}]$			> 70	
$\hat{E}_T^{\text{miss}} [\text{GeV}]$			> 200	
$p(\ell(1)), p(\ell(2))$		Set to zero after adding to E_T^{miss}		
N_{jet}			≥ 4	
$N_{b\text{-jets}}$			≥ 3	
$P(\text{Gbb})$	≥ 0.6	≥ 0.8	≥ 0.9	≥ 0.9
$\log_{10}(P(t\bar{t}))$	< -1.3	< -1.3	< -1.7	< -2.2
$\log_{10}(P(Z))$	≥ -3.0	≥ -2.7	≥ -4.9	≥ -3.7

Glino production in multi-b final states

26

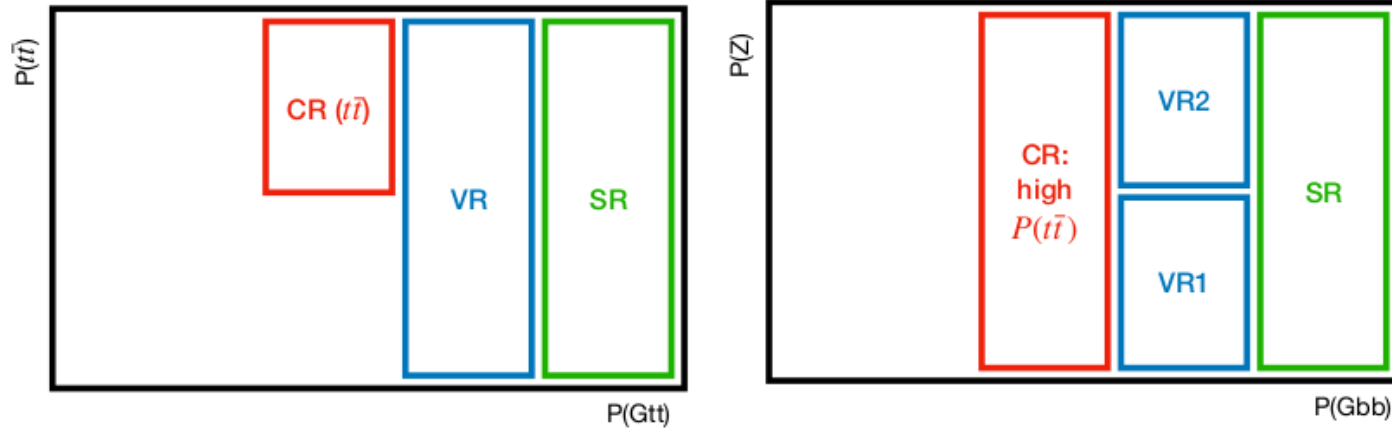


Figure 5: Schematic diagram of the inter-relationship of the SRs, $t\bar{t}$ CRs and VRs used in the NN analysis for the Gtt (left) and Gbb (right) SRs. The $t\bar{t}$ CRs and VRs apply additional selections to $\Delta\phi_{\min}^{4j}$, m_{eff} and M_J^Σ beyond those used in the SRs.

Gluino and squark production in multi-lepton final states

Table 1: List of Monte Carlo event generators and their settings for the main simulated samples of SM processes. When no reference is provided for the cross-section normalisation, the one computed by the generator is used. LO and NLO denote leading-order and next-to-leading-order calculations, respectively; in some cases (indicated), matrix elements are used with different accuracies depending on the number of additional parton emissions.

Process	Generator	Computation order	Parton shower	Cross-section normalisation	PDF set	Set of tuned parameters
$t\bar{t}W$ [64]	SHERPA 2.2.10 [65] + OPENLOOPS [68–70]	NLO 0-1j + LO 2j + LO $\mathcal{O}(\alpha^3 \alpha_s)$	CSSHOWER [66]	NLO	NNPDF3.0 _{NLO} [67]	default
$t\bar{t}\ell^+\ell^-$ [64] $1 < m_{\ell\ell} < 5 \text{ GeV}$	SHERPA 2.2.1 [65] MG5_AMC@NLO 2.3.3 [3]	NLO NLO	CSSHOWER [66, 71] PYTHIA 8.212 [72]	NLO NLO	NNPDF3.0 _{NLO} [67] NNPDF3.0 _{NLO} [67]	default A14 [73]
$t\bar{t}H$ [74]	POWHEG BOX v2 [65]	NLO	PYTHIA 8.230 [72]	NLO [75]	NNPDF3.0 _{NLO} [67]	A14 [73]
$t\bar{t}t\bar{t}$ [64]	MG5_AMC@NLO 2.3.3 [3] + MADSPIN [76, 77]	NLO	PYTHIA 8.230 [72]	NLO	NNPDF3.1 _{NLO} [67]	A14 [73]
Other $t/\bar{t} + X$ [64]	MG5_AMC@NLO 2.3.3 [3]	NLO or LO	PYTHIA 8.210-230 [72]	NLO or LO	NNPDF3.0/3.1 _{NLO} [67]	A14 [73]
Diboson [63]	SHERPA 2.2.2 [65] + OPENLOOPS [68–70]	NLO 0-1j + LO 2-3j	CSSHOWER [66, 71]	NLO	NNPDF3.0 _{NNLO} [67]	default
Triboson [63]	SHERPA 2.2.1 [65]	LO 0-1j	CSSHOWER [66, 71]	NLO	NNPDF3.0 _{NNLO} [67]	default
$t\bar{t}$ [78]	POWHEG BOX v2 [79–82]	NLO	PYTHIA 8.230 [83]	NNLO [78]	NNPDF3.0 _{NLO} [67]	A14 [73]
Single top (s -, t -channel) (tW)	POWHEG BOX v2 [80–82, 84] SHERPA 2.2.7 [65]	NLO NLO	PYTHIA 8.230 [83] CSSHOWER [66, 71]	NNLO [85, 86] NNLO + NNLL [87]	NNPDF3.0 _{NLO} [67] NNPDF3.0 _{NNLO} [67]	A14 [73] default
$W \rightarrow \ell\nu, Z/\gamma^* \rightarrow \ell\ell$ [88]	SHERPA 2.2.11 [65]	NLO 0-2j + LO 3-4j	CSSHOWER [66, 71]	NNLO [88, 89]	NNPDF3.0 _{NNLO} [67]	default

Gluino and squark production in multi-lepton final states

Table 2: Definition of the signal regions used for the RPC model shown in Figure 1(a), where pair production of gluinos leads to cascade decays of charginos into pairs of SM bosons.

SR name	$n_{\text{Sig}}(\ell)$ ($n_{\text{BL}}(\ell)$)	$n_{b\text{-jets}}$	n_{jets}	$p_{\text{T}}^{\text{jet}}$ [GeV]	$E_{\text{T}}^{\text{miss}}$ [GeV]	m_{eff} [GeV]	$\Delta\phi(\ell_1\ell_2, \mathbf{p}_{\text{T}}^{\text{miss}})$	$\mathcal{S}(E_{\text{T}}^{\text{miss}})$
SRGGWZ-L	≥ 2 (≥ 3)	= 0	≥ 6	> 25	> 200	$> 8 \times \sum p_{\text{T}}^{\ell}$	> 0.2	> 6
SRGGWZ-M	≥ 2 (-)		≥ 6	> 40	> 190	> 1300	> 0.8	-
SRGGWZ-H	≥ 2 (-)		≥ 6	> 40	> 150	> 2100	-	-

Table 3: Definition of the signal regions used for the RPC model shown in Figure 1(b), where pair production of squarks leads to cascade decays of charginos into pairs of SM bosons.

SR name	$n_{\text{Sig}}(\ell)$	$n_{b\text{-jets}}$	n_{jets}	$p_{\text{T}}^{\text{jet}}$ [GeV]	$E_{\text{T}}^{\text{miss}}$ [GeV]	m_{eff} [GeV]	$E_{\text{T}}^{\text{miss}} / \sum p_{\text{T}}^{\ell}$	$\sum p_{\text{T}}^{\ell} / \sum p_{\text{T}}^{\text{jet}}$	$n_{Z \rightarrow \ell^+ \ell^-}$
SRSSWZ-L	≥ 3	= 0	≥ 4	> 25	$> 0.2 \times m_{\text{eff}}$	-	-	< 0.2	$= 0^{\dagger}$
SRSSWZ-ML			≥ 6	> 25	> 150	> 800	> 1.2	< 0.3	$\geq 1^{\dagger}$
SRSSWZ-MH			≥ 5	> 40	> 200	> 900	> 1.1	< 0.4	$\geq 1^{\dagger}$
SRSSWZ-H			≥ 5	> 40	> 250	> 1500	> 0.3	< 0.7	-

† : based on number of SFOS pairs with $81 < m_{\text{SFOS}} < 101$ GeV

Gluino and squark production in multi-lepton final states

29

Table 4: Definition of the signal regions used for the RPC model shown in Figure 1(c), where pair production of gluinos leads to decays of charginos and neutralinos into sleptons.

SR name	$n_{\text{Sig}}(\ell)$	$n_{b\text{-jets}}$	n_{jets}	$p_{\text{T}}^{\text{jet}}$ [GeV]	$E_{\text{T}}^{\text{miss}}$ [GeV]	$E_{\text{T}}^{\text{miss}} / \sum p_{\text{T}}^{\text{jet}}$	$p_{\text{T}}^{\ell 2}$ [GeV]	Other
SRGGSlep-L	$\geq 3^{\dagger}$	= 0	≥ 4	≥ 40	–	> 0.4	> 30	$E_{\text{T}}^{\text{miss}} / \sum p_{\text{T}}^{\ell} > 1.4$
SRGGSlep-M					> 150	> 0.3	> 70	$\Delta\phi(\ell 1 \ell 2, \mathbf{p}_{\text{T}}^{\text{miss}}) > 0.7$
SRGGSlep-H					> 100	–	–	$\sum p_{\text{T}}^{\text{jet}} > 1200 \text{ GeV}$

† : SFOS pairs with $81 < m_{\text{SFOS}} < 101 \text{ GeV}$ are not allowed

Gluino and squark production in multi-lepton final states

Table 5: Definition of the signal regions used for the RPC model shown in Figure 1(d), where pair production of squarks leads to decays of charginos and neutralinos into sleptons. Requirements on p_T^ℓ apply to all three leptons.

SR name	$n_{\text{Sig}}(\ell)$	p_T^ℓ [GeV]	$n_{b\text{-jets}}$	n_{jets}	p_T^{jet} [GeV]	E_T^{miss} [GeV]	m_{eff} [GeV]	$\Delta\phi(\ell_1\ell_2, \mathbf{p}_T^{\text{miss}})$
	other requirements							
SRSSSlep-L	= 3*	< 60	= 0	≥ 3	> 60, 60, 25	> 100	> 600	> 1.4
	$\sum p_T^\ell / \sum p_T^{\text{jet}} < 0.6$							
SRSSSlep-ML	= 3*	> 30	= 0	≥ 3	> 60, 60, 25	> 100	> 700	> 1.4
	$E_T^{\text{miss}} / \sum p_T^\ell > 0.7, \sum p_T^\ell / \sum p_T^{\text{jet}} < 0.6$							
SRSSSlep-MH	= 3*	> 40	= 0	≥ 2	> 60	> 200	> 1000	> 0.5
	$E_T^{\text{miss}} / \sum p_T^\ell > 0.7, \Delta R(\ell_1, \ell_2) > 0.2$							
SRSSSlep-H	= 3*	> 40	= 0	≥ 2	> 60	> 200	> 2000	> 0.3
	$\Delta R(\ell_1, \ell_2) > 0.5$							
SRSSSlep-H (loose)	= 3*	> 40	= 0	≥ 2	> 60	> 200	> 1000	> 0.3
	$\Delta R(\ell_1, \ell_2) > 0.5$							

*: additional baseline leptons are not allowed, nor SFOS pairs with $81 < m_{\text{SFOS}} < 101$ GeV

Gluino and squark production in multi-lepton final states

Table 6: Definition of the signal region used for the RPV model shown in Figure 1(e), where the neutralino decays via the λ' RPV coupling of LQD type.

SR name	$n_{\text{Sig}}(\ell)$	$n_{b\text{-jets}}$	n_{jets}	$p_{\text{T}}^{\text{jet}}$ [GeV]	m_{eff} [GeV]
SRLQD	= 2	–	≥ 5	> 50	> 2600

Table 7: Definition of the signal regions used for the RPV model shown in Figure 1(f), where gluinos decay via top squarks and the λ'' RPV coupling of UDD type.

SR name	$n_{\text{Sig}}(\ell)$	$n_{b\text{-jets}}$	n_{jets}	$p_{\text{T}}^{\text{jet}}$ [GeV]	m_{eff} [GeV]	$\sum p_{\text{T}}^{\text{jet}}$ [GeV]
SRUDD-1b	= 2	= 1	≥ 6	> 50	–	> 1600
SRUDD-2b		= 2	≥ 2	> 25	–	> 1700
SRUDD-ge2b		≥ 2	≥ 5	> 50	–	> 1600
SRUDD-ge3b		≥ 3	≥ 4	> 50	> 1600	–

Gluino and squark production in multi-lepton final states

32

- Fake/non-prompt lepton background estimated with the matrix method.

$$\begin{pmatrix} n_{\text{signal}} \\ n_{\text{all}} \end{pmatrix} = \begin{pmatrix} 1 & 1 \\ \varepsilon^{-1} & \zeta^{-1} \end{pmatrix} \cdot \begin{pmatrix} n_{\text{signal, prompt}} \\ n_{\text{signal, F/NP}} \end{pmatrix} \leftarrow \text{the number we are after}$$

- Two samples, one with looser (baseline) lepton selection criteria.
- ε = efficiency for prompt lepton to pass signal lepton cuts.
 - Derived in simulated leptonic tt events.
- ζ = efficiency for fake/NP lepton to pass signal lepton cuts.
 - Measured in data for $10 < p_T < 75$ GeV, in regions enriched in tt events, with one or two prompt leptons and one F/NP lepton forming a same-sign pair.
 - Also the leading contribution of F/NP leptons to the SRs.
 - Separate measurements for events with ≤ 1 or ≥ 2 b-jets and cases where the electron satisfies the criteria to trigger.
 - WZ+jets and ttW contributions are scaled by the NFs (0.84 and 1.19) from CRs.
- The estimated contribution of charge-flip electrons is subtracted from all terms.

Gluino and squark production in multi-lepton final states

Table 8: The definitions of validation regions used to check the accuracy of the SM background predictions. Requirements are placed on signal leptons, jets, and some of the event-level variables defined in Section 6.

	$n_{\text{Sig}}(\ell)$	$n_{b\text{-jets}}$	n_{jets}	$p_{\text{T}}^{\text{jet}}$ [GeV]	m_{eff} [GeV]	$E_{\text{T}}^{\text{miss}}$ [GeV]
	other requirements					
VRWZ4j	= 3*	= 0	≥ 4	> 25	[600, 1500]	[30, 250]
	$E_{\text{T}}^{\text{miss}}/m_{\text{eff}} < 0.2$, $81 < m_{\text{SFOS}} < 101$ GeV					
VRWZ6j	= 3*	= 0	≥ 6	> 25	[400, 1500]	[30, 250]
	$E_{\text{T}}^{\text{miss}}/m_{\text{eff}} < 0.15$, $81 < m_{\text{SFOS}} < 101$ GeV					
VRTTV	≥ 2	≥ 1	≥ 3	> 40	[600, 1500]	[30, 250]
	$p_{\text{T}} > 30$ GeV for the two leading- p_{T} same-sign leptons, $\Delta R > 1.1$ between the leading- p_{T} lepton and any jet, $\sum p_{\text{T}}^{b\text{-jet}}/\sum p_{\text{T}}^{\text{jet}} > 0.4$, $E_{\text{T}}^{\text{miss}}/m_{\text{eff}} > 0.1$					
VRTTV1b6j	≥ 2	≥ 1	≥ 6	> 40	< 1500	[30, 250]
	$p_{\text{T}} > 30$ GeV for the two leading- p_{T} same-sign leptons, $E_{\text{T}}^{\text{miss}}/m_{\text{eff}} < 0.15$					
VRTTW	= 2* ($\mu^{\pm}\mu^{\pm}$)	≥ 2	≥ 2	> 25	< 1500	[30, 250]
	both leptons with $p_{\text{T}} > 25$ GeV, one with $p_{\text{T}} > 40$ GeV					
VRTTW3j	= 2* ($e^{\pm}\mu^{\pm}$)	≥ 2	≥ 3	> 25	< 1500	[30, 250]
	both leptons with $p_{\text{T}} > 25$ GeV					

*: additional baseline leptons are not allowed

Gluino and squark production in multi-lepton final states

Table 9: Fit configuration used to obtain the exclusion limits for each benchmark model. The targeted signal model is shown in the first column. The second and third columns show the signal regions and the fitted variable in each signal region, respectively. A statistical combination of signal regions is represented by the symbol ‘&’, while ‘||’ means that for each point of the $\{m_{\tilde{g}(\tilde{q})}, m_{\tilde{\chi}_1^0}\}$ parameter space, the signal region with the best expected sensitivity is chosen.

Model	Signal region(s)	Variable
$\tilde{g} \rightarrow qq'WZ\tilde{\chi}_1^0$ Figure 1(a)	SRGGWZ-L SRGGWZ-M SRGGWZ-H	single-bin, m_{eff} , single-bin
$\tilde{q} \rightarrow q'WZ\tilde{\chi}_1^0$ Figure 1(b)	SRSSWZ-L SRSSWZ-ML SRSSWZ-MH SRSSWZ-H	$E_{\text{T}}^{\text{miss}}, E_{\text{T}}^{\text{miss}}, m_{\text{eff}}, m_{\text{eff}}$
$\tilde{g} \rightarrow q\bar{q}(\ell\ell/\nu\nu)\tilde{\chi}_1^0$ Figure 1(c)	SRGGSlep-L SRGGSlep-M SRGGSlep-H	$E_{\text{T}}^{\text{miss}}/\sum p_{\text{T}}^{\ell}, E_{\text{T}}^{\text{miss}}, E_{\text{T}}^{\text{miss}}$
$\tilde{q} \rightarrow q(\ell\nu/\ell\ell/\nu\nu)\tilde{\chi}_1^0$ Figure 1(d)	SRSSSlep-L SRSSSlep-ML SRSSSlep-MH SRSSSlep-H (loose)	m_{eff}
$\tilde{g} \rightarrow q\bar{q}\tilde{\chi}_1^0, \tilde{\chi}_1^0 \rightarrow \ell qq$ Figure 1(e)	SRLQD	m_{eff}
$\tilde{g} \rightarrow \tilde{t}\tilde{t}, \tilde{t} \rightarrow \bar{b}\bar{d}$ Figure 1(f)	SRUDD-1b & SRUDD-ge2b	$\sum p_{\text{T}}^{\text{jet}}$

Stop production in $t\bar{t}+E_T^{\text{miss}}$ final states

Table 1: Overview of the configurations used to simulate signal and background processes.

Process	ME event generator	ME QCD accuracy	ME PDF	Parton shower and hadronisation	Cross-section calculation
SUSY signals	MADGRAPH 2.8.1, 2.9.9 [52]	0,1,2j@LO	NNPDF2.3LO	PYTHIA 8.240, 8.307	NNLO+NNLL [53–57]
DM signals	MADGRAPH 2.7.3	0,1j@LO	NNPDF2.3LO	PYTHIA 8.244	NLO [58, 59]
$t\bar{t}$	SHERPA 2.2.12 [60]	0,1j@NLO +2,3,4j@LO [74–77]	NNPDF3.0NNLO [61]	SHERPA [62–66]	NNLO+NNLL [67–73]
Single-top					
tW	POWHEG BOX v2 [78–81]	NLO	NNPDF3.0NLO	PYTHIA 8.307 [82]	NLO+NNLL [83, 84]
s- and t-channel	POWHEG BOX v2	NLO	NNPDF3.0NLO	PYTHIA 8.230	NLO [85, 86]
V +jets ($V = Z, W$)	SHERPA 2.2.11	0,1j@NLO +2,3,4j@LO	NNPDF3.0NNLO	SHERPA	NNLO [87]
$t\bar{t}V$	MADGRAPH5_AMC@NLO 2.3.3 [52]	NLO	NNPDF3.0NLO	PYTHIA 8.210	NLO QCD+EW [88]
VV'	SHERPA 2.2.1, 2.2.2	0,1j@NLO+2,3j@LO	NNPDF3.0NNLO	SHERPA	

- $t\bar{t}$ now simulated with Sherpa (used to be PowHeg) → better high- p_T modelling.
- The tW sample now uses dynamic renormalization and factorization scales ($\mu_F=\mu_R=H_T/2$).
 - Greatly improves modelling of the $t\bar{t}$ and tW interference.
 - The difference between the diagram removal (DR) and diagram subtraction (DS) schemes is greatly reduced. → Reduced single top uncertainty and NF closer to unity.

Stop production in $t\bar{t}+E_T^{\text{miss}}$ final states

Table 2: Summary of the selections for each event category together with the definitions of the hadronic and leptonic top quark candidates. Trigger, lepton and E_T^{miss} selections are described in the text. Large- R jets are referred to as ‘LR’ for brevity.

Analysis Category	High- E_T^{miss}		Boosted					
	1b	2b	1b-lep-0t	1b-had-0t	2b-0t	1b-lep-1t	1b-had-1t	2b-1t
$N(\text{LR jet})$	0		≥ 1					
$N(\text{top-tagged LR jet})$	-		0			≥ 1		
$N_{b\text{-jet}}$ with $\Delta R(b, \text{LR jet}) < 1.1$	-		0	≥ 1	≥ 1	0	≥ 1	≥ 1
$N_{b\text{-jet}}$ with $\Delta R(b, \text{LR jet}) > 1.1$	-		≥ 1	0	≥ 1	≥ 1	0	≥ 1
top-NN-tagged multiplet	✓		-					
$N_{b\text{-jet}}$	1	≥ 2	-					
$N_{\text{light-jet}}$	≥ 2	≥ 1	-					
top _{had} candidate	top-NN multiplet		LR jet					
top _{lep} candidate	$\ell + j$	$\ell + b$	$\ell + b$	$\ell(+j)$	$\ell + b$	$\ell + b$	$\ell(+j)$	$\ell + b$
Event NN selection	See Table 3							

Stop production in $t\bar{t}+E_T^{\text{miss}}$ final states

37

Table 3: Summary of the selections on the stop-NN and DM-NN output values which define CRs, VRs and SRs. Signal efficiency in SRs are also reported. They are computed as the fraction of signal events in a given category with a NN output value in the range accepted in the SR. The quoted range is based on efficiencies estimated for all signals across the simulated parameter space. In boosted categories, only efficiencies for $\tilde{t}_1\tilde{t}_1$ signals with $\Delta m(\tilde{t}_1, \tilde{\chi}_1^0) > 500$ GeV are considered.

Category	stop-NN				DM-NN			
	CR Range	VR Range	SR Range	Eff.	CR Range	VR Range	SR Range	Eff.
High- E_T^{miss} 1b	[0.2, 0.64[[0.64, 0.79[[0.79, 1.0]	0.4-0.9	[0.3, 0.69[[0.69, 0.87[[0.87, 1.0]	0.3-0.4
High- E_T^{miss} 2b	[0.1, 0.56[[0.56, 0.7[[0.7, 1.0]	0.5-0.9	[0.3, 0.6[[0.6, 0.76[[0.76, 1.0]	0.6-0.8
Boosted 1b-lep-1t	[0, 0.65[[0.65, 0.8[[0.8, 1.0]	0.5-0.9				
Boosted 1b-had-1t	[0, 0.65[[0.65, 0.85[[0.85, 1.0]	0.6-0.9				
Boosted 2b-1t	[0, 0.75[[0.75, 0.95[[0.95, 1.0]	0.6-0.8				
Boosted 1b-lep-0t	[0, 0.7[[0.7, 0.85[[0.85, 1.0]	0.6-0.8				
Boosted 1b-had-0t	[0.1, 0.75[[0.75, 0.95[[0.95, 1.0]	0.4-0.8				
Boosted 2b-0t	[0, 0.65[[0.65, 0.8[[0.8, 1.0]	0.6-0.9				

Stop production in $t\bar{t}+E_T^{\text{miss}}$ final states

38

Table 4: Summary of the statistical model in terms of event categories, regions into which categories are divided, observables used in the template fit and normalisation factors (‘NFs’) applied to background contributions in each region. ‘NN’ stands for the NN output value. The background process on which these NFs act is indicated by the name of the NF. All ten CRs and eight SRs are used in the fit for the $\tilde{t}_1\tilde{t}_1$ search. The statistical model for the $t\bar{t}+\text{DM}$ search differs as the SRs in the boosted categories are not used.

Category	Fitted observable		Normalisation Factors						
	CR	SR	NF _{top-1L} ^{High-met}	NF _{top-1L} ^{Boosted}	NF _{top-2L} ^{High-met}	NF _{top-2L} ^{Boosted}	NF _W ^{High-met}	NF _W ^{Boosted}	NF _{singletop}
High- E_T^{miss} 1b	$m_T \times q(\ell)$	NN	✓		✓			✓	✓
High- E_T^{miss} 2b	$m_T \times q(\ell)$	NN	✓		✓			✓	✓
Boosted 1b-lep-1t	$m_T \times q(\ell)$	NN		✓		✓		✓	✓
Boosted 1b-had-1t	$m_T \times q(\ell)$	NN		✓		✓		✓	✓
Boosted 2b-1t	$m_T \times q(\ell)$ (low- m_{T2}) Yield (high- m_{T2})	NN		✓		✓		✓	✓
Boosted 1b-lep-0t	$m_T \times q(\ell)$	NN		✓		✓		✓	✓
Boosted 1b-had-0t	$m_T \times q(\ell)$	NN		✓		✓		✓	✓
Boosted 2b-0t	$m_T \times q(\ell)$ (low- m_{T2}) Yield (high- m_{T2})	NN		✓		✓		✓	✓

Stop production in $t\bar{t}+E_T^{\text{miss}}$ final states

39

Table 5: Ratios of the signal cross sections as determined in the fit to the expected signal cross sections $\mu = \sigma_{\text{fit}}^{\text{sig}} / \sigma_{\text{Th}}^{\text{sig}}$ for different signal models in the $\tilde{t}_1\tilde{t}_1$ and $t\bar{t}+\text{DM}$ searches. Components of the total uncertainty $\sigma(\mu)$ from statistical and major systematic uncertainties are also shown. The component from statistical uncertainties in data is estimated as the uncertainty on μ when all nuisance parameters in the fit are fixed. Components from systematic uncertainties are estimated as $\sigma_{\text{sys}}(\mu) = \sqrt{\sigma^2(\mu) - \sigma_{\text{fix}}^2(\mu)}$, where $\sigma_{\text{fix}}(\mu)$ is the uncertainty when the nuisance parameters associated to the systematic uncertainties are fixed. The components are reported as percentage relative to the total uncertainty $\sigma(\mu)$. Correlations across components are not accounted for.

	$\tilde{t}_1\tilde{t}_1, m(\tilde{t}_1, \tilde{\chi}_1^0)$ GeV		$t\bar{t}+\text{DM}, m(a, \chi)$ GeV	
	(1000, 600)	(1200, 200)	(50, 1)	(200, 1)
$\mu \pm \sigma(\mu)$ (total uncertainty)	0.27 ± 0.4	0.9 ± 0.5	0.14 ± 0.10	0.22 ± 0.18
Data statistical uncertainty	85 %	91 %	72 %	72 %
Background modelling	42 %	33 %	52 %	50 %
MC statistical uncertainty	24 %	23 %	31 %	36 %
Jet energy scale and resolution	21 %	13 %	29 %	28 %
Flavour tagging efficiency	17 %	11 %	20 %	19 %

Stop production in $t\bar{t}+E_T^{\text{miss}}$ final states

40

Table 18: Lists of input features for the stop- and DM-NNs in each event category. Inputs are defined in text. † The p_T of the $t\bar{t} + E_T^{\text{miss}}$ system is before Lorentz boost.

Category	High- E_T^{miss}		Boosted		
	1b	2b	1b-lep-1t (-0t)	1b-had-1t (-0t)	2b-1t (-0t)
E_T^{miss}	E	✓	✓	✓	✓
	Significance	✓	✓	✓	✓
top_{had}	p_x	✓	✓	✓	✓
	p_y	✓	✓	✓	✓
	p_z	✓	✓	✓	✓
	E	✓	✓	✓	✓
	top-NN output	✓	✓		
top_{lep}	p_z	✓	✓	✓	✓
	E	✓	✓	✓	✓
$t\bar{t} + E_T^{\text{miss}}$	p_T †	✓	✓	✓	✓
	lepton				
b -jet in top_{had}	p_x	✓	✓	✓	✓
	p_y	✓	✓	✓	✓
	p_z	✓	✓	✓	✓
	E	✓	✓	✓	✓
	E	✓	✓	✓	✓
b -jet in top_{lep}	p_x	✓	✓	✓	✓
	p_y	✓	✓	✓	✓
	p_z	✓	✓	✓	✓
	E	✓	✓	✓	✓
	E	✓	✓	✓	✓
$\Delta R(b, b)$	✓	✓	✓	✓	✓
$m_T(\ell, E_T^{\text{miss}})$	✓	✓	✓	✓	✓
$m_{T2}(b, b, E_T^{\text{miss}})$	✓	✓			
$m_{T2, \text{min}}(b + \ell, b, E_T^{\text{miss}})$	✓	✓			